

**Specific Absorption Rate (SAR) Analysis Using Finite  
Difference Time Domain (FDTD) Computation  
on behalf of Hi-tronics Designs, Inc.  
for the Angel Medical Systems Guardian IMD Model AG101  
(Implantable Medical Device)**

**The analysis has been performed by Remcom Inc.**

**David C. Carpenter PhD.**

**March 10, 2006**

## ***Introduction***

Hi-tronics Designs, Inc. (HDI) has developed an Implantable Medical Device (IMD) which has the capability of wirelessly transmitting data to/from a patient/physician. The RF communication system utilizes the MICS band (Medical Implant Communications Service). The amount of radiated power transmitted through the human body tissue using this technology may be defined by a measure known as SAR (Specific Absorption Rate). Values of SAR that can be safely used in these applications have been defined by the ANSI/IEEE and are part of the FCC guidelines for medical implant communications.

Certification of medical-implant transmitters under the FCC Part 95 Medical Implant Communication Services (MICS) requires a calculation using Finite Difference Time Domain (FDTD) analysis of the SAR associated with the presence of a radio frequency (RF) transmitter. This report details the SAR analysis of the RF transmitter used in the Angel Medical Systems (AMS) Guardian IMD.

## ***Summary***

The commercial software analysis package XFDTD, a finite difference time domain analysis of the electromagnetic fields has been used to calculate the electromagnetic fields produced by the IMD and the resulting SAR (specific absorption rate) in human body tissue. The model used an accurate representation of the IMD and the HiFi Body Mesh available with the XFDTD Software.

The results are as follows:

Maximum SAR value	674 mW/kg
Maximum 1g average SAR value	73 mW/kg
Maximum 10g average SAR value	22 mW/kg
Average SAR value in torso	18 $\mu$ W/kg

**Table 1: Summary of SAR results from analysis**

The ANSI C95-1-1992 limit is 1.6 W/kg. In this study, the computed value of the maximum 1g average is 73 mW/kg. The level of computed SAR is 4.5% of the limit stated in the specification.

These FDTD results show that the HDI IMD can safely be used in its intended application with respect to the energy emitted during normal operation.

## ***Method of Analysis***

The software used for the simulation, modeling and analysis was XFDTD v6.3. A 3D CAD model of the IMD was supplied by HDI in SAT format. This is the generic format used by the modeling system within XFDTD. The material specification was obtained from HDI and the electromagnetic properties of the device were either supplied by HDI or obtained from published data. The specific values are provided in Appendix A. The CAD model and mesh model used in this analysis are shown in Figure 1. Figures 1c and 1d show the antenna and lead adapter detail of the model. Figure 1d also shows the source voltage model that has been used to excite the antenna. Dimensions of the final mesh model where cross referenced to those described in the IMD users manual and found to be accurate to within 1 cell size (0.5mm).

The HiFi Body Mesh supplied with XFDTD was used to model the human tissues and body structure for this analysis. This model included frequency dependent electromagnetic properties of human tissues such that the correct values may be automatically selected to match the frequency of interest. In this case the frequency was 402.5 MHz, which is within the narrow operating frequency of the IMD (FCC MICS Band of 402 MHz to 405 MHz).

The Human Body mesh was loaded first and the cell size set to 5mm. This matches the resolution of the tissue data within the HiFi Body Model. An initial mesh was generated to include only the Human Body. The IMD CAD model was then imported and positioned in the appropriate location (comparable to a pacemaker) within the Human Body Model. The cell size in the region of the IMD was then reduced to 0.5mm, using the built-in adaptive meshing features in XFDTD. This proved to be adequate to resolve the features of the IMD. From experience, it has become clear that the SAR is highest in the region of the antenna and so the Body Model was then limited to include only the torso to simplify computations and reduce simulation time.

The IMD was placed in the left area chest region, 33 mm below the chest skin (surface), 75 mm to the left of the spine and 160 mm down from the top of the shoulder. Figure 2 illustrates the location.

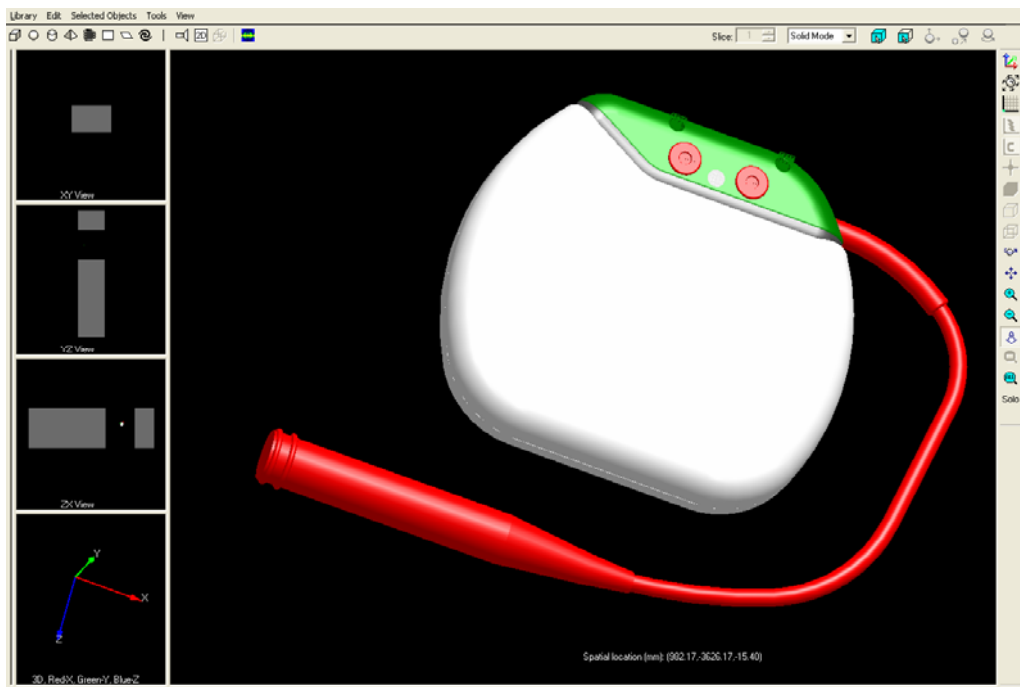


**Figure 1a: 3D CAD model of IMD**

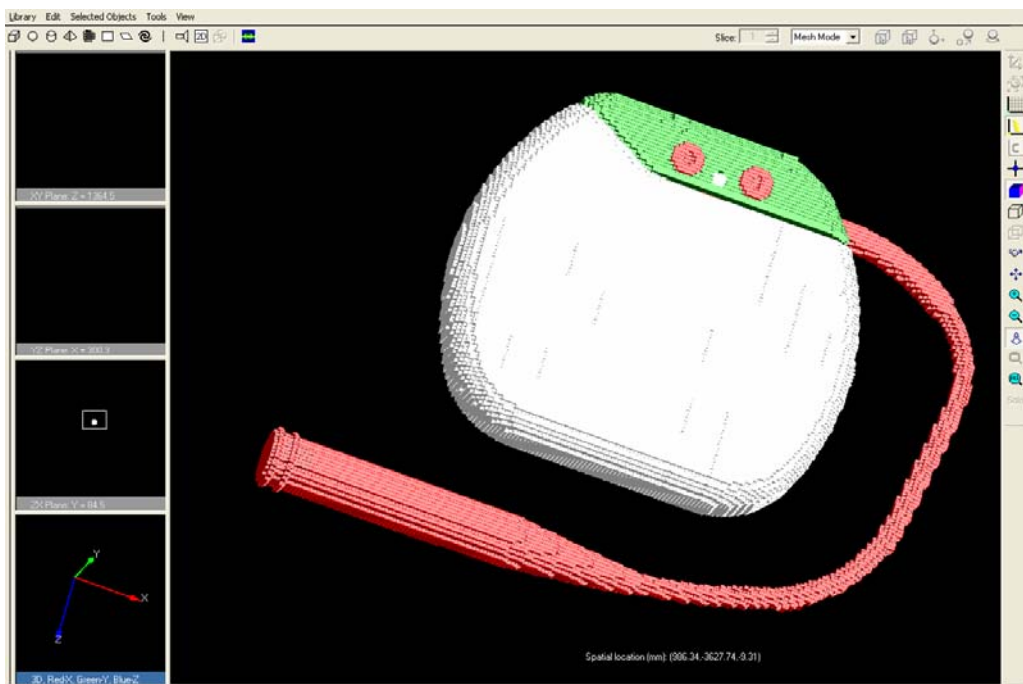


**Figure 1b: FDTD 3D Mesh model of IMD**

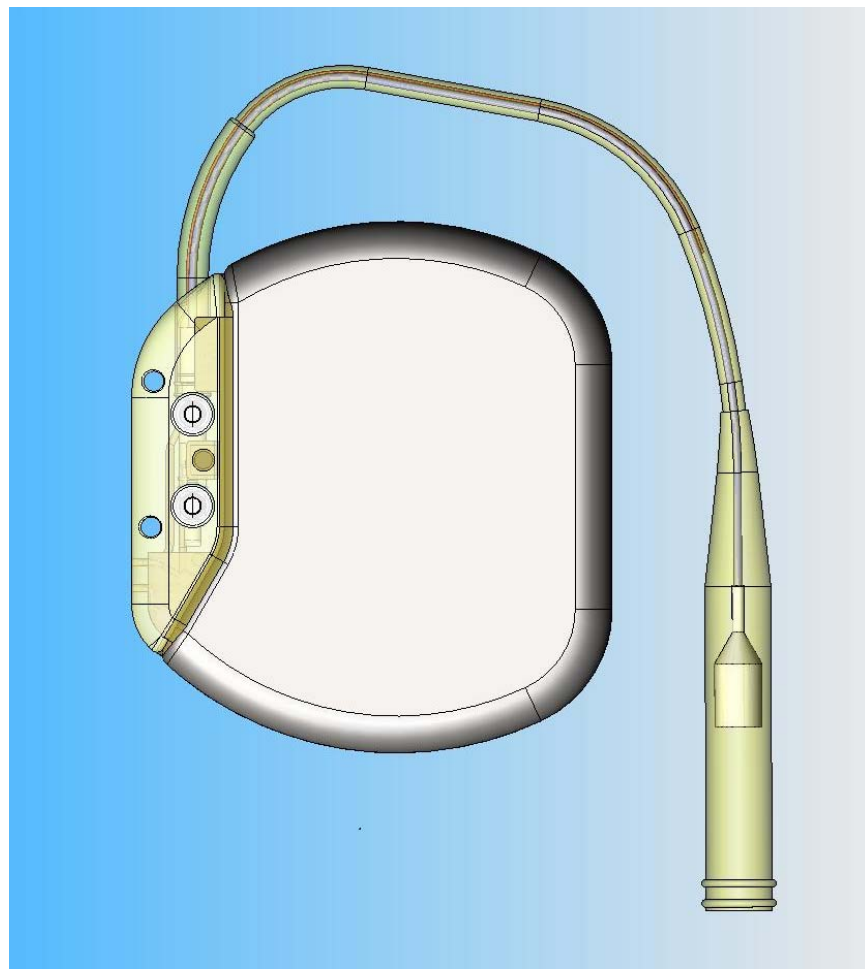


**Figure 1c: Parts display of IMD**

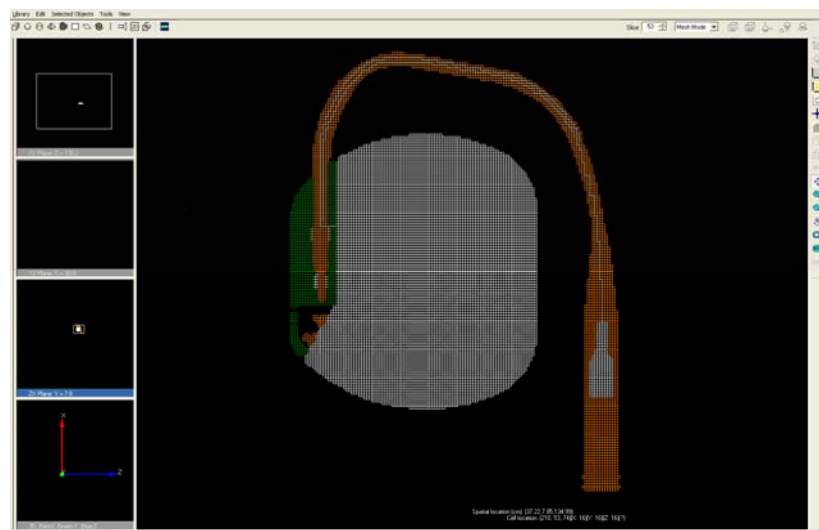


**Figure 1d: Section through mesh model of IMD**

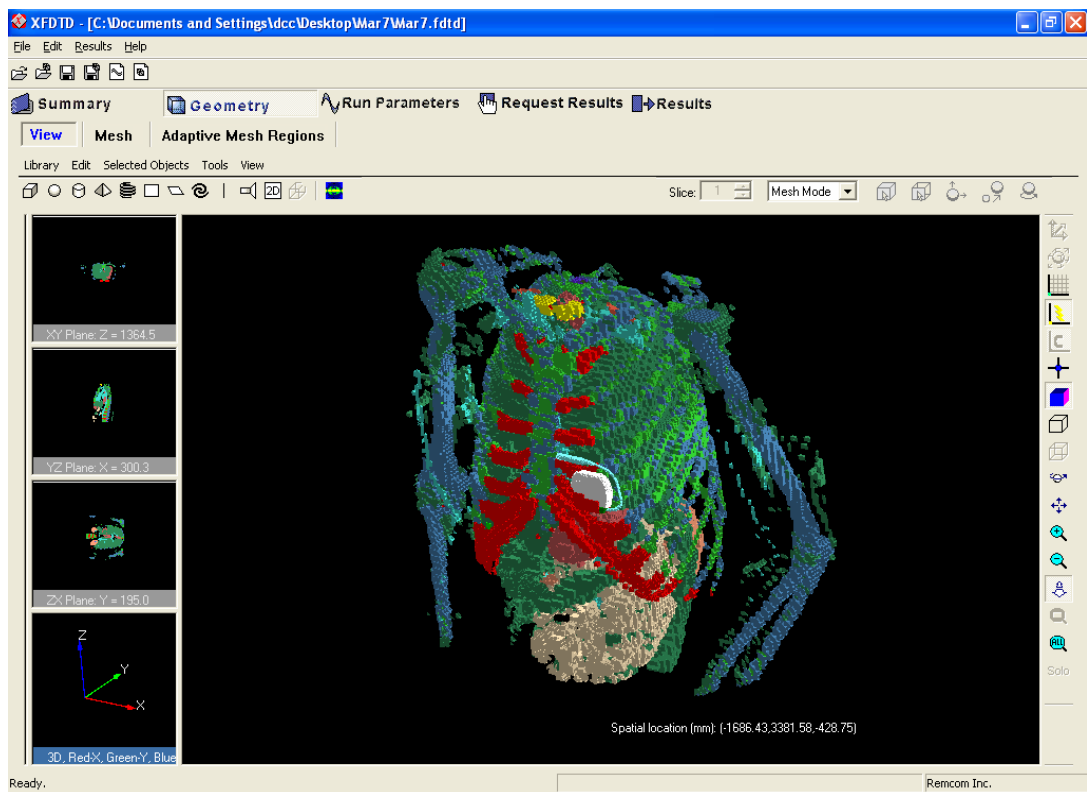
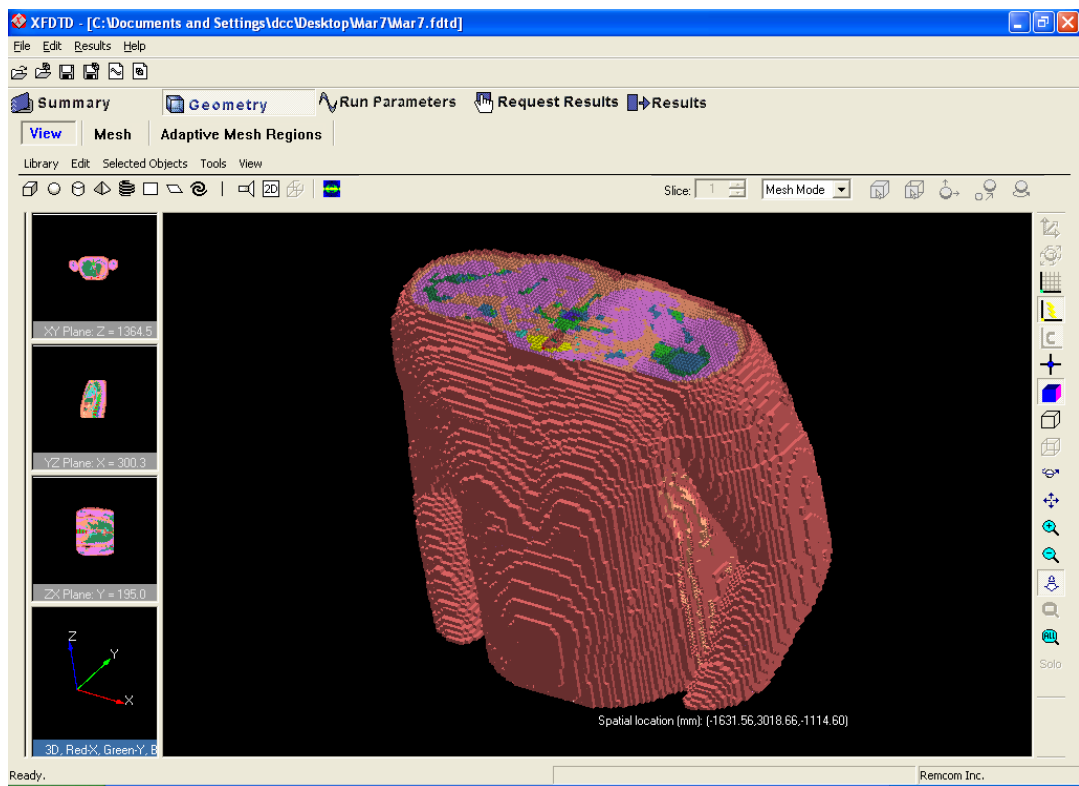


**Figure 2: Torso biological tissue model (full model and selected tissues shown)  
With IMD in place**

A single frequency analysis was carried out at 402.5 MHz, which is expected to be representative of the narrow band of MICS operation (402 MHz – 405 MHz).

XFDTD provides post processing features that allow SAR statistics to be calculated at a single frequency. The body tissue electromagnetic properties data have been determined by using a series of single pole Lorentz equations to fit published measured data to these equations. The equations are in the form of:

$$\epsilon(\omega) = \epsilon_{\infty} + (\epsilon_s - \epsilon_{\infty}) \frac{\omega_0^2}{\omega_0^2 + 2j\omega\tau_0 - \omega^2}$$

Where  $\epsilon_{\infty}$  is the infinite frequency permittivity

$\epsilon_s$  is the static frequency permittivity

$\tau_0$  is the relaxation time (s)

$\omega$  is the frequency (radians/s)

In the region of 402.5MHz, this represents a slowly changing permittivity and conductivity. Thus it is reasonable to expect similar SAR results over the narrow band of operation of the IMD.

The SAR values are calculated from the following equation:

$$SAR = \frac{\sigma_x |E_x|^2}{2\rho_x} + \frac{\sigma_y |E_y|^2}{2\rho_y} + \frac{\sigma_z |E_z|^2}{2\rho_z}$$

where

SAR – Specific Absorption Rate (W/kg)

$\sigma_{x,y,z}$  - electrical conductivity (S/m)

$|E_{x,y,z}|$  - magnitude of electric field (V/m)

$\rho_{x,y,z}$  - material density (kg/m<sup>3</sup>)

## **Results of SAR Analysis**

XFDTD provides results in a tabulated format and as distributed field and SAR values in planes of the model.

Figure 3 shows a 3D view of the SAR distribution in the x-y plane where the value of 1 gm average SAR is a maximum. Figure 4 shows a more detailed view of this. The maximum value was computed as 73 mW/kg.

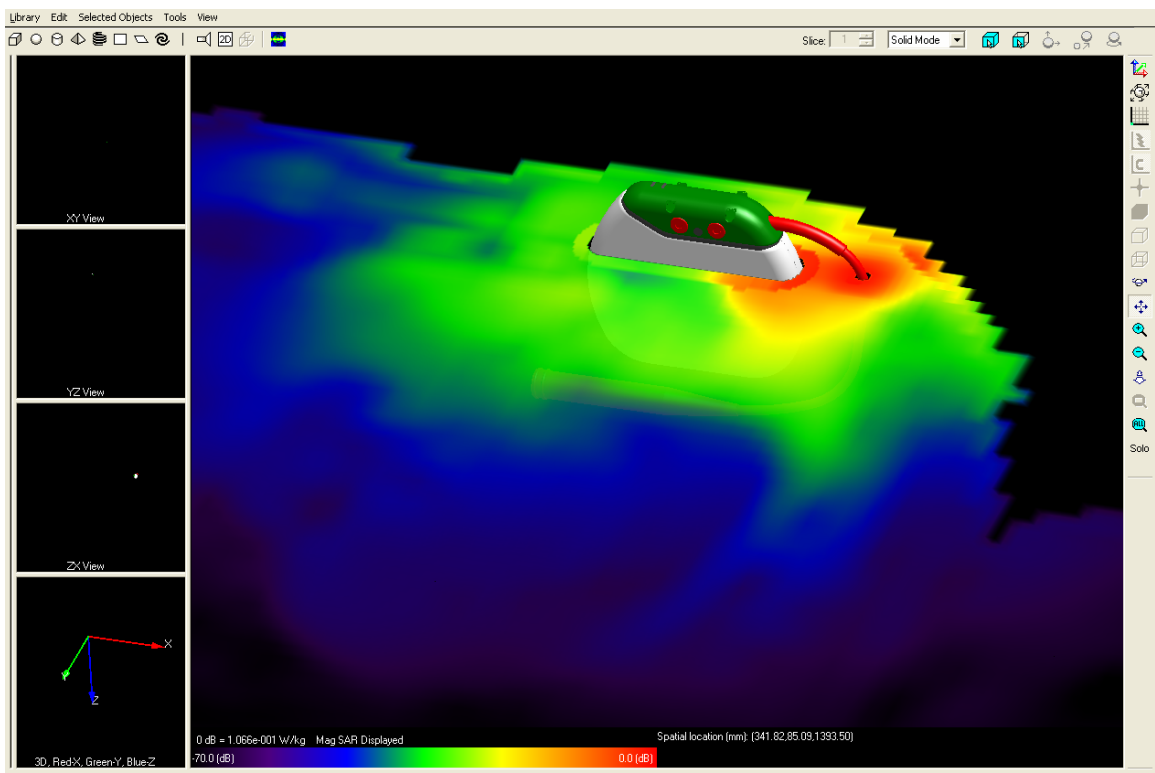


**Figure 3: 3D view of the SAR distribution at the maximum value**

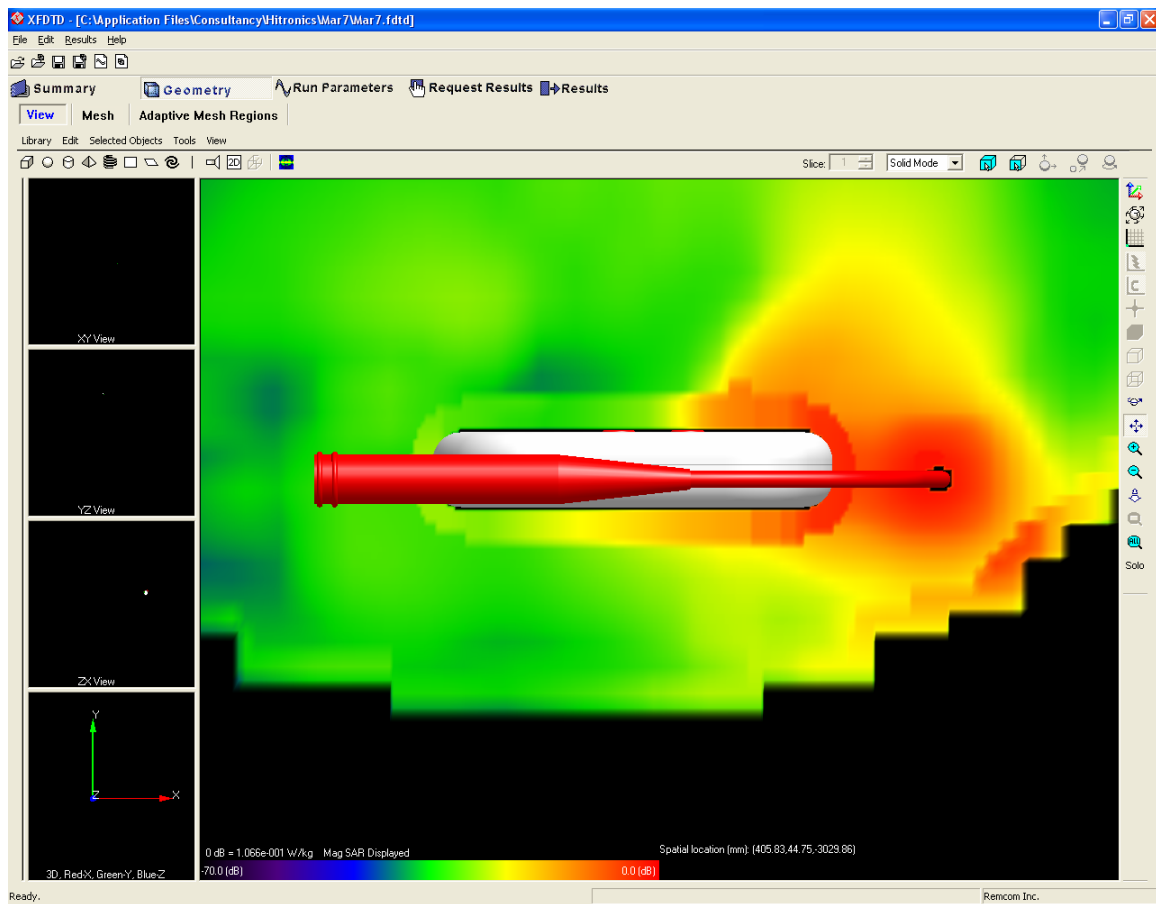


**Figure 4: 2D view of the SAR distribution with and without geometry**

The statistics table generated by XFDTD v6.3 is given in Figure 5.

SAR Statistics	
Maximum SAR (W/kg):	6.7425e-001
Maximum SAR Position (x,y,z):	(259.51,114)
	( 397.00, 78.00, 1384.00 ) (mm)
Average SAR in exposed Object	1.8239e-005
Maximum 1 g Average SAR (W/kg):	7.2561e-002
Maximum 1 g Average SAR Position (x,y,z):	(265.50,123)
	( 400.00, 77.50, 1388.50 ) (mm)
Maximum 10 g Average SAR (W/kg):	2.2403e-002
Maximum 10 g Average SAR Position (x,y,z):	(231.40,103)
	( 383.00, 70.15, 1378.50 ) (mm)
Computed Net Input Power (W):	1.3653e-003
Scaled Net Input Power (W):	9.2900e-004
<input type="button" value="Close"/>	

**Figure 5: SAR Summary Table Generated by XFDTD**

The statistics table of Figure 5 combined with the SAR distribution of Figure 4 shows that the maximum SAR value is located very close to the IMD Lead Adapter that contains the antenna and falls away within a few millimeters of the Lead Adapter/Antenna assembly. This confirms that using a torso only model is valid.

### **Conclusions**

The Finite Element Difference Time Domain analysis has shown that the SAR values produced by the radiated RF power of the AMS Guardian IMD are well below the maximum levels set by the ANSI/IEEE standards incorporated into the FCC guidelines for MICS. The results show that the computed maximum 1g average SAR value is 13.4dB below the maximum level permitted by the guidelines.

## ***Computational Resources***

### *Hardware and Software:*

For geometric modeling and post processing (creating and editing the model, view and calculating results):

Dell dual 2.66GHz processor Windows XP Professional Workstation, 2GB RAM

For running the analysis:

Atipa 32 processor Linux cluster, Myrinet internal LAN with 1GB RAM per processor

Software:

XFDTD Bio-Pro v6.3 with adaptive meshing and HiFi Body mesh model.

### *Computational Requirements:*

FDTD is a computationally intensive method and most reasonable calculations will need a fast computer and several hundred megabytes of computer memory. For most applications it is fairly simple to estimate the amount of computer memory required for a calculation. The most important factor for the memory usage, and in large part the run time, is the number of FDTD cells used to represent the structure under test. Each FDTD cell has six field values associated with it: three electric fields and three magnetic fields. Additionally each cell has six flags associated with it to indicate the material type present at each of the six field locations. The field values are real numbers, each four bytes in length, while the flags are each one byte. This gives a memory usage per FDTD cell of 24 bytes for fields and 6 bytes for flags for a total of 30 bytes. An estimate of the total memory required, in bytes, is obtained by multiply the number of FDTD cells by the 30 bytes per cell value. There is some overhead in the calculation, but it is generally quite small.

Estimating the execution time of an FDTD calculation is more complicated since performance of computer processors varies. One method of estimating is to compute the total number of operations to be performed. There are about 80 operations per cell, per time step during the FDTD calculations. The total number of operations is found from the product of the number of cells, the number of time steps, and the factor of 80 operations per cell, per time step. If a value of the floating-point performance of the processor is known, a value for execution time can be computed.

The HiFi Body mesh supplied with XFDTDv6.3 has a resolution of 5mm cell size and body tissue data. This cell size was used for regions of the model that did not include the geometry of the IMD. Reducing the cell size in these regions (i.e. increasing the mesh density) would not increase the accuracy of the model as the tissue material representation would not change (since this data only has a resolution of 5mm).

In the region of the IMD (implanted in the HiFi Body Model), mesh resolution was tested at 2mm, 1mm, 0.5mm and 0.2mm using the adaptive mesh feature of XFDTDv6.3. It was found that the IMD was not well represented using 2mm cell sizes. The results for further refinements in the adaptive mesh were as follows:

Adaptive cell size (mm)	1g average SAR (W/kg)	1g average SAR location: x, y, z (cm)	10g average SAR (W/kg)	10g average SAR location (cm)
1	0.065	39, 8, 142	0.017	39, 8, 142
0.5	0.072	40, 8, 139	0.002	38, 7, 138
0.2	0.064	40, 8, 142	0.017	38, 7, 141

**Table 2: Variation of SAR with adaptive cell size**

To ensure the IMD geometry was well defined, an adaptive cell size of 0.5mm was chosen. From the tests carried out, this gave the worst case SAR result. The variation in the 1g averaged SAR with adaptive cell size changed from 1mm to 0.2mm is shown to be  $\pm 5\%$ .

### ***FDTD Algorithm implementation, validation and steady state termination procedures***

FDTD solves Maxwell's equations in the time domain. This means that the calculation of the electromagnetic field values progresses at discrete steps in time. One benefit of the time domain approach is that it gives broadband output from a single execution of the program.

FDTD has also been identified as the preferred method for performing electromagnetic simulations for biological effects from wireless devices [1]. The FDTD method has been shown to be the most efficient approach and provides accurate results of the field penetration into biological tissues [2, 3]. From these studies, the variation between measurement and calculation in computing 1g average SAR has been shown to be a maximum of 3% at the frequency of interest.

In the FDTD approach, both space and time are divided into discrete segments. Space is segmented into box-shaped “cells”, which are small compared to the wavelength. The electric fields are located on the edges of the box and the magnetic fields are positioned on the faces as shown in Figure 6. This orientation of the fields is known as the Yee cell [4] and is the basis for FDTD.

Time is quantized into small steps where each step represents the time required for the field to travel from one cell to the next. Given the offset in space of the magnetic fields from the electric fields, the values of the field with respect to time are also offset. The electric and magnetic fields are updated using a leapfrog scheme where first the electric fields, then the magnetic are computed at each step in time.

When many FDTD cells are combined together to form a three-dimensional volume, the result is an FDTD grid or mesh. Each FDTD cell will overlap edges and faces with its neighbors, so by convention each cell will have three electric fields that begin at a common node associated with it. The electric fields at the other nine edges of the FDTD cell will belong to other, adjacent cells. Each cell will also have three magnetic fields originating on the faces of the cell adjacent to the common node of the electric fields as shown in Figure 6.

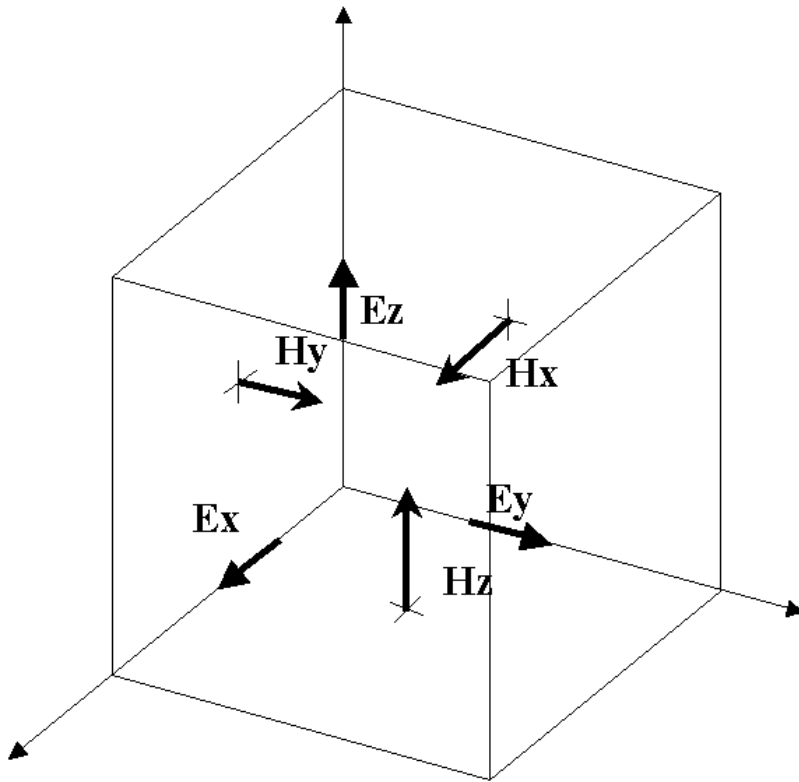


**Figure 6: The Yee cell with labeled field components.**

Within the mesh, materials such as conductors or dielectrics can be added by changing the equations for computing the fields at given locations. For example, to add a perfectly conducting wire segment to a cell edge, the equation for computing the electric field can be replaced by simply setting the field to zero since the electric field in a perfect conductor is identically zero. By joining numerous end-to-end cell edges defined as perfectly conducting material, a wire can be formed. Introducing other materials or other configurations is handled in a similar manner and each may be applied to either the electric or magnetic fields depending on the characteristics of the material. By associating many cell edges with materials, a geometrical structure can be formed within the FDTD

grid such as the dielectric sphere shown in Figure 7. Each small box shown in the figure represents one FDTD cell.

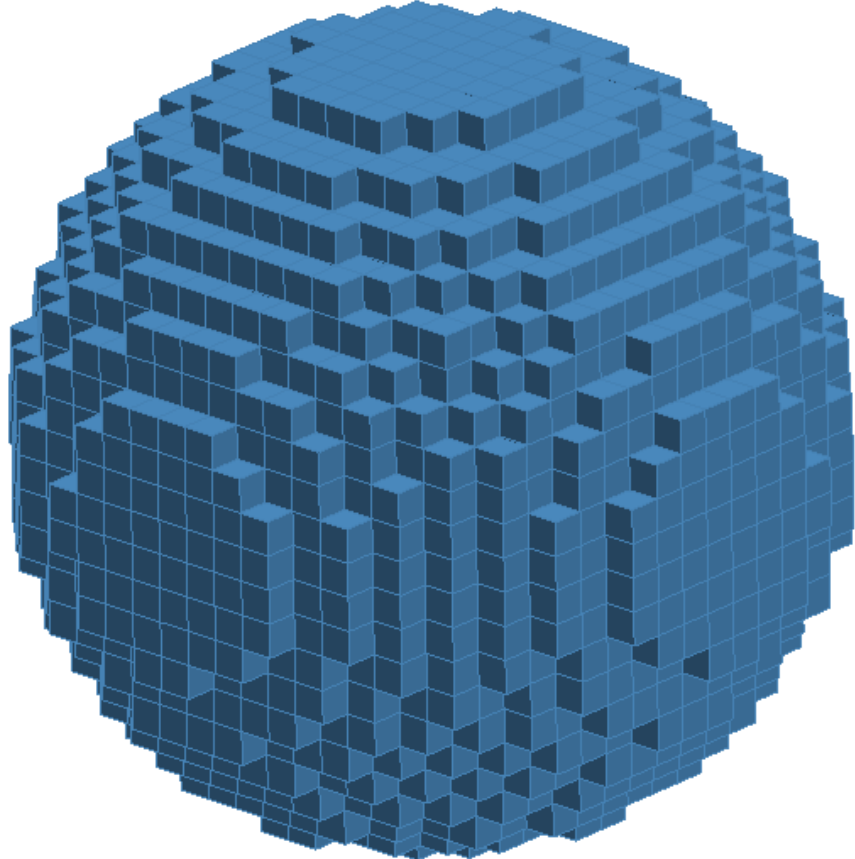


**Figure 7: A dielectric sphere as meshed in an FDTD grid.**  
**The individual cell edges (electric field locations) are displayed as the overlapping grid lines.**

The cell size, the dimensions of the box, is the most important constraint in any FDTD simulation since it determines not only the step size in time, but also the upper frequency limit for the calculation. A general rule of thumb sets the minimum resolution, and thus the upper frequency limit, at ten cells per wavelength. In this case, the cell size is set by dimensions and features of the IMD.

An excitation is applied to the FDTD simulation by applying a sampled waveform to the field update equation at one or several locations. At each step in time, the value of the waveform over that time period is added into the field value. The surrounding fields will propagate the introduced waveform throughout the FDTD grid appropriately, depending on the characteristics of each cell. A calculation must continue until a state of convergence has been reached. This typically means that a steady-state condition has

been reached where the peak fields everywhere in space vary by less than -40dB). For this analysis, convergence occurred after 17416 time steps.

FDTD is capable of simulating a wide variety of electric and magnetic materials. All FDTD cells are initialized as free space and the fields at all cell edges are updated using the free space equations unless another material is added to replace the free space.

Perfectly conducting electric (PEC) and magnetic (PMC) materials are simulated by setting the electric or magnetic field to zero for any cell edges located within these materials. Because of the simplicity of the calculation for these materials, it is better to use a perfect conductor rather than a real conductor whenever feasible. It has been shown that using these types of conditions, compared to using measured material data, for highly conductive materials (such as copper or Titanium) the difference in results is negligible (<< 1%).

Frequency independent dielectric and magnetic materials, considered “normal” materials by XFDTD, are defined by their constitutive parameters of relative permittivity and conductivity for the electrical material, or relative permeability and magnetic conductivity for the magnetic material.

Where the frequency independent material is not appropriate for broadband calculations, a frequency dependent, or dispersive, material should be substituted. Some common examples of frequency dependent materials are high water content materials such as human tissues, and metals when excited at optical frequencies. Included in XFDTD is the capability to simulate electric and magnetic Debye and Drude materials such as plasmas, Lorentz materials, and anisotropic magnetic ferrites, as well as frequency independent anisotropic dielectrics, and nonlinear diagonally anisotropic dielectrics. The usage of these materials in XFDTD is in other documents [5].

A sinusoidal source is used for the steady-state output required here as Specific Absorption Rate (SAR) is required.

A three-dimensional grid of cells forms the XFDTD geometry and the fields updated at every cell location are dependent on the neighboring fields. However, due to memory limitations the grid must end at some point and because of this, the fields on the outer edges of the grid cannot be updated correctly. To correct this situation, outer radiation boundary conditions are applied at the edges of the XFDTD grid.

The outer radiation boundary is a method for absorbing fields propagating from the XFDTD grid toward the boundary. By absorbing these fields, the grid appears to extend forever. The performance of the outer boundaries is an important factor in the accuracy of an FDTD calculation and care should be taken to correctly use them.

In some cases a reflecting boundary rather than an absorbing one is preferred. A perfectly conducting boundary (either electric or magnetic) [6] may be used to image the fields in an FDTD calculation.

## ***Computational Parameters***

Cell Size	5mm base cell size with 0.5mm adaptive mesh
Domain size	800mm x 610mm x 750mm
Time Step	963 fs
Tissue Separation from ABCs	$\geq 20$ cells

**Table 2: Summary of model computational parameters**

## ***Biological model***

The tissue material data used in the study has been obtained from work by Camilia Gabriel [7]. Since the material parameters are dispersive, a 3 pole drude model has been used to fit to the cole-cole equation used with Gabriel's data [7].

The physical position of tissues are determined by using the HiFi Body model provided with XFDTDv6.3. This model was created from the Visible Human Project with enhancements from high resolution MRI measurements. This Visible Human Project digitized the tissue locations of the body by taking a donated frozen cadaver and removing 5mm slices from the body. By color photography, each slice was used to identify tissues such as skin, muscle, blood vessels etc. The HiFi Body model uses 23 types of tissue data as shown in Table 3. This HiFi Body Phantom supplied with XFDTD has been used for many similar studies and has been shown to be valid in these cases, examples are given here [8, 9].

## ***Heterogeneous Human Head and Body Meshes***

The initial meshes were converted directly from the data generated by the Visible Human Project sponsored by the National Library of Medicine (NLM). The initial XFDTD meshes were created by a conversion program followed by visual examination of the data with help from [10] and [11]. The resulting meshes were later reviewed and revised by Dr. Michael Smith and Mr. Chris Collins of the Hershey Medical Center, Hershey, PA. These revisions included improved fidelity, additional shoulder region, and removal of small regions of blood which do not correspond to a living human, but pooled after the death of the human subject. Before any calculation involving the human head or body meshes, the tissue parameters are adjusted to the desired frequency of the calculation.

## ***HiFi Male Body Mesh***

The Remcom High-Fidelity Male Body Mesh is based on the data from the Visible Human Project. It uses 5x5x5 mm cells and has dimensions 136 x 87 x 397 for 4,697304 cells. The High-Fidelity mesh contains 23 materials which are assigned as follows:

Description	Conductivity (S/m)	Relative Permittivity
#2 Skin	0.561875	41.9613
#3 Tendon, pancreas, prostate, aorta, liver	0.743688	50.9544
#4 Fat/Yellow Marrow	0.0441352	5.06915
#5 Cortical Bone	0.108259	13.5939
#6 Cancellous Bone	0.22267	21.2369
#7 Blood	1.71207	57.4585
#8 Muscle, heart, spleen, colon, tongue	0.96977	64.1191
#9 Grey Matter, cerebellum	0.867293	54.9298
#10 White Matter	0.524866	40.3333
#11 Cerebro-spinal fluid	2.31207	69.0096
#12 Sclera/Cornea	1.03188	54.9156
#13 Vitreous Humor	1.55207	68.3793
#14 Bladder	0.304666	17.7086
#15 Nerve	0.492073	36.0963
#16 Cartilage	0.642073	44.1077
#18 Gall Bladder bile	1.59905	76.91
#19 Thyroid	0.806958	60.2915
#20 Stomach, Esophagus	1.11453	74.8356
#21 Lung	0.704385	52.9279
#22 Kidney	1.14183	57.8985
#24 Testes	1.12	65.66
#25 Lens	0.692813	52.3372
#27 Small intestine	2.03429	74.7797

**Table 3: Tissue data used in analysis**

Measured values for the tissue parameters for a broad frequency range from 1KHz to 20GHz are included with the mesh data. The tissue parameters may be adjusted automatically for a specific frequency, in this case 402.5 MHz. The correct values from the table of measured data are selected or interpolated and entered into the appropriate mesh variables. The mesh must be saved after adjusting the parameters for the new values to be used in the XFDTD calculation but the parameters can be adjusted as many times as required.

#### *Specific Absorption Rates (SARs) and Averaging*

SAR is defined in terms of the root mean square (RMS) of the electric field magnitude by the relation

$$\mathbf{SAR} = (\sigma |E|^2)/\rho$$

Here sigma ( $\sigma$ ) is the electrical conductivity (S/m) and rho ( $\rho$ ) is the material density (defined in kg/m<sup>3</sup> in XFDTD). Since the FDTD grid defines the electric fields at the edges of the cells, a single SAR value is formed by summing and averaging the

contributions of the 12 electric fields on the edges of the cells. The SAR is then referenced to the center of the FDTD cell.

In XFDTD the SAR may only be computed with a sinusoidal excitation and in normal dielectric materials. Frequency dependent materials have a loss term formed by the imaginary part of the permittivity rather than simply by the conductivity, and are not supported for SAR calculations.

The SAR values are saved only in complete voxels (closed FDTD cells) where all 12 edges of the cell are lossy dielectric material (non-zero conductivity) with a non-zero density. To exclude certain materials from a SAR calculation, simply leave the material density as zero.

Planes of SAR values may be saved in XFDTD. Following the calculation, the unaveraged SAR data is available as field plots which may be displayed over the geometry. Generally the unaveraged SAR values are of less importance than the averaged SARs. The unaveraged SAR is a function of the FDTD mesh size, so the values can change dramatically when the same geometry is simply meshed in a grid with a different cell size.

A more important unit is the averaged SAR. The average is computed over cubical volumes of voxels (FDTD cells) where no face of the averaging volume is external to the body and thus full of air (or other non-tissue material). In certain cases, particularly at the surface of the body, the cubical volume rule can not be satisfied. In those situations, special rules exist for setting the SAR value in a given voxel [12].

Often the SAR values might only be of interest in a small region of the XFDTD geometry. In such cases, it is not necessary to compute the average SAR values over the entire geometry. Rather, save single unaveraged SAR planes around the region of interest and perform the averaging through the interface in post processing. Care must be taken to ensure that a sufficient number of unaveraged SAR planes are stored to form value averaging volumes. For example, in a one centimeter FDTD mesh, a single voxel of tissue (with a mass density of water) will have a mass of one gram. At a minimum, a region of 3x3x3 voxels will be necessary to form a volume with enough mass to enclose 10 grams. So, at least three unaveraged SAR planes are required. If the cell size is 1mm, then a region of 23x23x23 cells is needed to enclose 10 grams, so in that case at least 23 unaveraged SAR slices must be saved.

### *Frequency Dependent Material Parameters Human Meshes*

Many biological calculations such as SAR are performed at a single frequency, so the electrical parameters of the tissues are single values valid only for that frequency. In general, the material parameters for human tissue vary significantly with frequency, so broad band calculations are difficult to perform accurately when the tissue parameters are set for only a single frequency. Measurements and mathematical models of the frequency response of the human tissues have been performed and developed, and XFDTD has a special, multipole frequency-dependent setting for including human tissues in broad band

calculations. This wide band human body model is especially useful for cases where pulse inputs are desired, such as when the broad band result is required.

As an example, consider the plot of the mathematical model of relative permittivity for cortical bone tissue shown in Figure 8. Over the frequency range from about 50MHz up to 20GHz, the relative permittivity changes significantly from a peak of nearly 16 down to 6. Also shown in Figure 8 is the approximated curve fit used in XFDTD for simulating the tissue which provides a good match over the entire frequency range. As compared to the single frequency permittivity at 1 GHz, the response of the tissue will clearly be different.

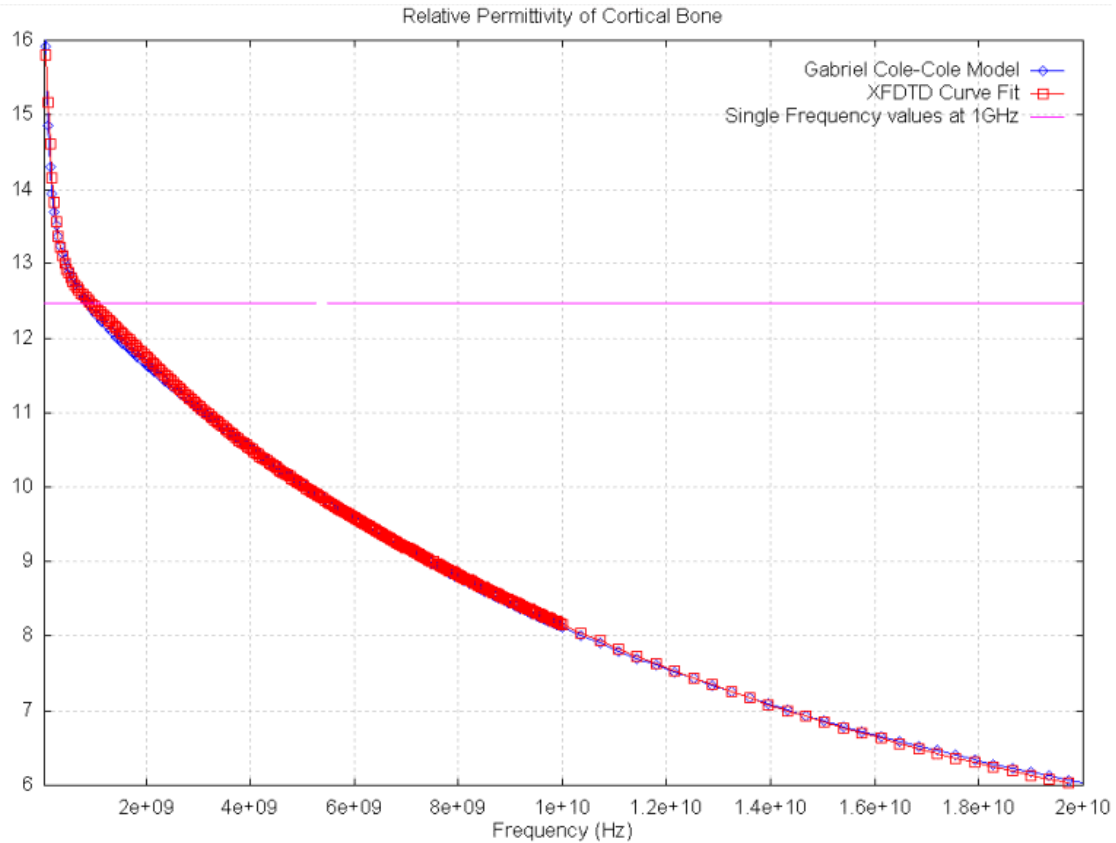


**Figure 8: Plot of the relative permittivity of cortical bone tissue as a function of frequency.**

### ***Limitations***

The Finite Element Difference Time Domain analysis has been based on information, data, measurements and specifications provided by HDI. Remcom Inc. are not responsible for effects on the results of this analysis due to incorrect information, data measurements or specifications provided by HDI.

## **Appendix A:**

### *Specifications of IMD:*

Peak power delivered to antenna (measurement supplied by HDI): 4dBm or 2.51mW. The measurements varied from 2.7dBm to 3.91 dBm. Hence using a value of 4 dBm gives a worst case value and the level of SAR calculate in this analysis can be expected to vary by -25%.

RF Tx Duty cycle of device when RF operating: 37% of “on-time” which occurs during full data upload

Mean power delivered to antenna: 0.929mW

### *Material properties of IMD:*

Header: Bionate 75D, conductivity=0 S/m, relative permittivity = 3.7, permeability=1.

All conducting parts (titanium can, header blocks, screws and antenna) were treated as PEC (perfect electrical conductors). Experience has shown that the difference between using PEC and the actual conductivity of highly conductive metallic parts is negligible.

Lead adapter insulation and other similar parts: Silicone, conductivity=0 S/m, relative permittivity = 3.2, permeability=1.

## References

1. IEEE publication C95.3 "Recommended Practice for Measurements and Computations with Respect to Human Exposure to Radio Frequency Electromagnetic Fields, 100kHz to 300GHz")
2. <http://www.remcom.com/examples/xfdtdexampleDetailUpdated.php?exampleID=77&thisProduct=XFDTD60>
3. <http://www.remcom.com/examples/xfdtdexampleDetailUpdated.php?exampleID=71&thisProduct=>
4. Yee, K. S., "Numerical Solution of Initial Boundary Value Problems Involving Maxwell's Equations in Isotropic Media," IEEE Transactions on Antennas and Propagation, vol. AP-17, pp. 585-589, May 1966.
5. XFDTD v6.3 Reference Manual.
6. J.P. Berenger, "A perfectly matched layer for the absorption of electromagnetic waves," J. Computat. Phys., Oct. 1994.
7. <http://www.brooks.af.mil/AFRL/HED/hedr/reports/dielectric/Report/Report.html>
8. Specific Absorption Rate (SAR) Analysis Using Finite Difference Time Domain Computation for RF Transmitter Circuit Employed in Biotronik Lexos "T" Implantable Cardiac Defibrillators, October 7, 2003.
9. FDTD for Bioelectromagnetics: Modeling MICS Implant in the Human Body. Dr Piotr Przybyszewski and Chris Fuller, Medtronic Inc., September 3, 2003.
10. Robert S. Ledlet, H. K. Huang, and John C. Mazziotta, "CrossSection Anatomy An Atlas for Computerized Tomography," The Williams and Wilkins Co., 1977
11. Richard A. Boolootian, "Elements of Human Anatomy and Physiology," West Publishing Co., 1976
12. C95.3.2002, "Recommended Practice for Measurements and Computations with Respect to Human Exposure to Radio Frequency Electromagnetic Fields, 100kHz to 300GHz", IEEE Standards and Coordinating Committee 28 on Non-Ionizing Radiation Hazards, April 2002.